Design of Micro-Scale Fuel Processors Assisted by Numerical Modeling

Chunshe Cao, Yong Wang, Jamie D. Holladay, Evan O. Jones, and Daniel R. Palo
Pacific Northwest National Laboratory, Richland, WA 99352

DOI 10.1002/aic.10364
Published online in Wiley InterScience (www.interscience.wiley.com).

Computer-aided design (CAD) of a micro-scale fuel processor is described. Transport phenomena and reaction processes in a methanol steam reformer and a selective carbon monoxide methanator have been mathematically illustrated with a three-dimensional pseudo-homogeneous model based on fundamental conservation laws of mass and energy. Simulations provide carbon conversion as well as local temperature distributions in the micro-scale fuel processors. Various reactor design options were evaluated by such numerical modeling predictions. The tailored temperature profile in the optimized reactor configuration and process conditions give high efficiency in generating low-CO–content hydrogen-rich gas stream for miniature fuel cell applications. © 2005 American Institute of Chemical Engineers *AIChE J,* 51: 982–988, 2005
Keywords: modeling, micro-scale fuel processor, steam reforming, methanol, methanation

Introduction

Remotely and autooperated microelectronic devices are often used for applications in the area of intelligence, military, industrial sensoring, and meteorology. These miniature devices usually require high energy density and a long-duration power supply. However, current battery technology does not provide the energy densities needed to sustain power for extended periods.[1-3] Even advanced lithium (Li)-ion battery technology can produce an energy density of only 0.15 $kW_e \cdot h \cdot kg^{-1}$.[1] Additionally, as advances are made in the development of electronic devices, adding functionality and new features, the power they require continues to increase. This severely limits the available run time of these devices when operating on small batteries. Li-ion technology falls far short of the required energy density for most applications. In contrast, the energy density associated with a typical hydrocarbon fuel such as methanol is nearly 20 times that of Li-ion battery technology.[3] Recent advances in fuel cells and fuel reforming have enabled the efficient use of methanol and other liquid fuels as energy sources for small devices, with the potential to replace the lower-energy density batteries currently in use. Even a diluted liquid fuel has higher energy density than that of typical batteries produced by current technology.[3,4]

Although it is clear that liquid fuels hold a significant advantage over batteries in terms of energy density, battery power has the advantages of being much more mature and having no moving parts. This is where the challenge lies. If liquid fuels are ever to replace battery power to a significant extent, systems must be developed that take advantage of the high energy density of liquid fuels without adding undue complexity, size, weight, or maintenance. Under a project sponsored by the Defense Advanced Research Projects Agency (DARPA) and carried out by Battelle Pacific Northwest National Laboratory, we have developed a relatively simple and small power system that harnesses the energy of a liquid fuel like methanol and converts it to electricity. For this technology, methanol was selected as the hydrogen source also because of its "sweetness" (sulfur free) and readiness of being activated at relatively low temperature (under 250°C). Low-temperature operation in such a miniature power device reduces heat loss and insulation, thus improving the power density of the entire system. In addition, low-temperature reforming offers the potential to generate less carbon monoxide that causes potential poisoning of the fuel

Correspondence concerning this article should be addressed to C. Cao at chunshe.cao@pnl.gov.

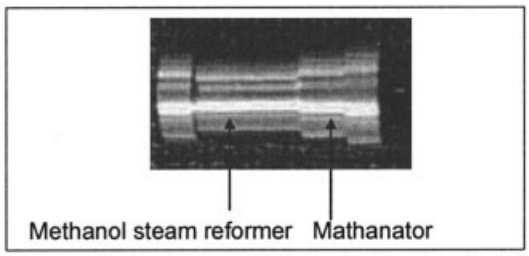

Figure 1. Micro-scale fuel processor.

cell electrodes. This micro fuel processor (Figure 1) was integrated with a small fuel cell (1 to 2 cm^2) and successfully produced up to300-mW_e power.[5]

Such a fuel processor is expected to be self-sustained without external heating. Thus design of the reactor with thermally high efficiency is important. An endothermic catalytic steam reforming reaction and fuel vaporization are the major heat sinks of the whole system. The local cold spots in the reforming section substantially reduce the reaction rate and force the system running at longer residence time or higher temperature to achieve a high conversion level. However, high-temperature operation can affect catalyst performance such as high CO selectivity and shortened catalyst life, and also cause more heat loss to the environment. Therefore, understanding the temperature distribution within the catalytic reactor helps to optimize the reactor design and operating conditions. Another issue that arises when developing and testing reactors on this size scale is the measurement and control of temperatures within the device. Because the steam reforming devices are so small, sufficient room for thermocouples or other measurement devices is just not available. Furthermore, the size of the measurement instrument relative to the device it is monitoring is such that significant heat conduction occurs, decreasing the thermal efficiency of the device and altering its performance. For these reasons, an accurate model is necessary for proper reactor design and optimization. In particular, knowing the temperature profile in the device helps to adjust reactor design and operation parameters to allow catalysts to "see" their desired temperatures. Such a model yields useful data that could not be acquired empirically. This paper describes the modeling work conducted for the development project to assist fuel reformer design and optimization, which leads to improved performance.

Experimental and Modeling

The integrated micro fuel processor incorporates three catalytic sections: methanol steam reforming for hydrogen production, methanol combustion to supply the heat for the endothermic reaction of steam reforming and fuel vaporization, and methanation to reduce carbon monoxide concentration. The primary chemical reactions are represented as follows:

(1) Steam reforming

$$CH_3OH + 1.2H_2O \rightarrow CO + CO_2 + H_2 \quad \Delta H_r = 56 \text{ kJ/mol}$$

(2) Combustion

$$CH_3OH + 1.5O_2 \rightarrow CO_2 + 2H_2O \qquad \Delta H_r = -676 \text{ kJ/mol}$$

(3) Methanation

$$CO + 3H_2 \rightarrow CH_4 + H_2O \qquad \Delta H_r = -206 \text{ kJ/mol}$$

$$CO_2 + 4H_2 \rightarrow CH_4 + 2H_2O \qquad \Delta H_r = -165 \text{ kJ/mol}$$

The reactor body is made of stainless steel. The total volume of the fuel processor is less than 0.3 cm^3 and the device weighs less than 1 g. Figure 2 shows the steam reforming and CO-cleanup sections of the processor. The premixed liquid methanol and water (steam to carbon molar ratio = 1.2) were fed and vaporized in a small tube on the axis of the catalyst annular bed. The reactant gaseous mixture is then radially distributed by a porous disk and flows through the catalyst bed countercurrently against the liquid feed, in which conversion takes place. The heat required for the steam reforming reaction is continuously supplied by conduction from the combustion chamber below the disk. The reformate mixture is sequentially fed into the in situ methanator for CO reduction. Supported Pd/ZnO on Al_2O_3 was used as the methanol steam reforming catalyst[6-8] and 3%Ru on γ-Al_2O_3 as methanation catalyst. The mean diameter of the catalyst particles was 200 μm. Methanol steam reformer has 14 mg catalyst loading and the methanation bed consists of 13 mg catalyst. A 0.25-mm-OD thermocouple was inserted into the combustion reactor to monitor the operating temperature. Another thermocouple was attached to the reforming end measuring temperature at the feed tube entrance. The flow rate of the methanol–water mixture was varied from 0.03 to 0.2 cm^3/h. Methanol also serves as the fuel to the combustion reactor, into which liquid methanol flow rate ranged from 0.1 to 0.5 cm^3/h and air flow rate 10–25 sccm. The gaseous products were analyzed with an on-line gas chromatograph (Agilent QuadH) as well as an infrared CO gas analyzer (ZRH, California Analytic Instruments).

A three-dimensional pseudo-homogeneous model was formulated based on the first principles of material and energy balance for the catalytic reactions of methanol steam reforming and selective CO methanation. The model was constructed on the FEMLAB platform[9] where the parameters for different processes, such as steam reforming, methanation, and heat transfer in the insulation layer, were assigned within their geometrical subdomains. Convection–diffusion and convection–conduction modules in the FEMLAB library were used as two multiphysics representing mass and heat transfer. The

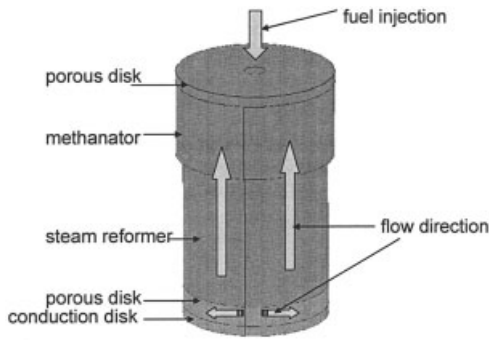

Figure 2. Integrated methanol steam reformer and CO cleanup section in a micro-power fuel processor.

Table 1. Parameter Values Used in the Simulation*

Reactor Module	Average Gas Density ρ at Operating Conditions (kg/m^3)	Heat Capacity of Gas Mixture, C_p (J kg^{-1} mol^{-1})	Effective Thermal Conductivity, k_{eff} (W/m-K)	Effective Diffusivity, D_{eff} (cm^2/s)
Steam reformer	0.44	1710	0.22	0.00456
Methanator	0.37	1965	0.2	0.00340

*Conditions: P = 1 atm, $T_{combustion}$ = 300°C, liquid fuel flow rate = 0.05 cm^3/h, steam/C = 1.2.

following general partial differential equations govern all the process domains but containing specific coefficients

$$\nabla \cdot (-D_{eff}\nabla c) + \vec{u} \cdot \nabla c = R \tag{1}$$

$$\nabla \cdot (-k_{eff}\nabla T) + \rho C_p \vec{u} \cdot \nabla T = R(-\Delta H_r) \tag{2}$$

where R is the disappearing rate of the key component (MeOH or CO), which is a function of component concentration c (or partial pressure p) and temperature T; ΔH_r is the heat of reaction; k_{eff} is the effective conductivity of the catalyst bed; D_{eff} is the effective diffusivity; and $\vec{u}$ is linear velocity. The effective diffusivity is contributed by molecular diffusion, Knudsen diffusion, and catalyst structures such as bed density and tortuosity. They were calculated using molecular kinetics theory.[10] This pseudo-homogeneous model assumes that the variations of such parameters bed effective diffusivity, effective thermal conductivity, velocity, and heat capacity are small, and the axial thermal conduction and diffusion are negligible. Moreover, a typical linear flow velocity is 5 mm/s in such a small reactor, which corresponds to a Reynolds number of about 0.4 with a creeping flow pattern. Uniform velocity distribution in the radial direction was assumed for model simplification. Typical parameter values used in the simulation are listed in Table 1.

The reaction rate of methanol steam reforming was determined by independent kinetic measurement with the same catalyst in a microchannel reactor. The methanol disappearing rate was reported in our previous publication,[6] which was correlated with its partial pressure, steam partial pressure, and temperature. The activity of selective methanation catalyst was measured by a microfixed bed reactor in which catalysts were diluted with SiC particles for isothermal (SiC/Cat = 3). The inlet mixture containing 0.8% CO, 20.4% CO_2, 57.3%, H_2, and 21.5% H_2O simulates a reformate composition. The reaction rate was empirically correlated with the first-order kinetics to CO with the frequency of 1.8639×10^{18} mol g_{cat}^{-1} s^{-1} and the activation energy of 143 kJ/mol.

Fuel vaporization in the hollow tube at the reactor axis was treated as a boundary condition to the catalyst domains (both steam reforming and methanation).

$$q(z) = -k_{eff}\left.\frac{\partial T}{\partial r}\right|_{r=r_0} \tag{3}$$

where r_0 is the feed tube diameter. Because the fuel mixture vaporizes immediately at the area of the injection point in the operating temperature range (270–320°C), the location of the fuel injection port will alter the flux distribution $q(z)$ as a design option. A polynomial form or a step function can be used to represent such distribution. The total flux was constrained by the liquid mixture flow rate and the average operating temperature. In the simulation practice, the polynomial order was chosen by fitting the measured temperature difference between the two thermocouples. Therefore, the boundary conditions for perfect insulation around the reactor cylinder are as follows:

$$T(z = 0) = T_0 \tag{4}$$

$$\left.\frac{\partial T}{\partial r}\right|_{r=d/2} = 0 \tag{5}$$

$$\left.\frac{\partial T}{\partial z}\right|_{z=L} = 0 \tag{6}$$

$$q(z) = -k_{eff}\left.\frac{\partial T}{\partial r}\right|_{r=r_0} \tag{3}$$

where r_0 is the feed tube diameter, d is the catalyst bed diameter, L is the bed length, and $q(z)$ is the heat flux arising from vaporization. When insulation material is incorporated into the model, the domain Eq. 2 for energy balance is reduced to a simple conduction equation

$$k_{insulation}\nabla^2 T = 0 \tag{7}$$

and the boundary condition (Eq. 5) has been changed to

$$k_{insulation}\left.\frac{\partial T}{\partial r}\right|_{r=d'/2} = h(T - T_{ambient}) \tag{8}$$

where $k_{insulation}$ is the thermal conductivity of the insulation material and h is the convective heat transfer coefficient between the insulation materials and the atmosphere. An empirical value of h was chosen to be 5 W m^{-2} K^{-1}.[11] The coupled PDEs (Eqs. 1, 2, or 7) in different domains with boundary conditions 3–6 and 8 were numerically solved with FEMLAB in which the cylindrical coordinates were used.

Results and Discussion

The model was first applied to an adiabatic methanol steam reforming reactor to reveal its temperature distribution. The simulation results were not only used to determine the temperature gradients in the catalyst bed but also to evaluate the design options of the fuel injector. In the methanol steam reforming reactor, the catalyst bed boundaries were insulated except for an isothermal heat conduction disk on the bottom. Figure 3 shows the temperature profile in the steam reforming catalyst pellet at the conditions corresponding to 80 mW_e power output. The coordinate scales on the graph, in millimeters, represent the actual dimensions of the reactor. The fuel injection port was at the entrance of the feeding tube. It can be seen that the temperature is higher in the lower portion of the catalyst pellet. This is in contrast to the usual temperature

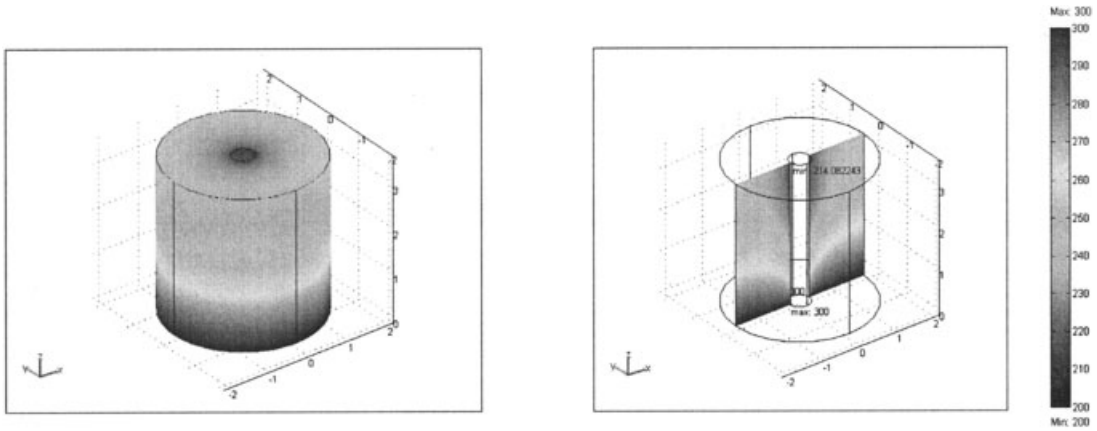

Figure 3. Temperature distribution in a micro-scale methanol steam reformer with an entrance fuel injection.

Conditions: temperature in °C, "adiabatic mode"; $T_{combustion}$ = 300°C, liquid fuel flow rate = 0.05 cm^3/h, steam/C = 1.2.

distribution in a conventional fixed-bed reactor, given that a high carbon conversion rate occurs with high methanol partial pressure when the reactant stream first comes into contact with the catalyst. The significant endotherm of hydrocarbon steam reforming has been mitigated by the heat transfer from the combustion chamber. The cross section of the catalyst pellet shown in Figure 3 also shows that the temperature is lower in the center of the catalyst pellet. In the axial direction, the temperature drops sharply within the entrance region of the liquid feeding tube, caused by the large latent heat of rapid liquid fuel vaporization. The maximum temperature difference in the reformer has been found to be 86°C throughout the entire reformer. A 100% overall methanol conversion was achieved at a weight hourly space velocity of 1.84 $g_{MeOH}\ g_{cat}^{-1}\ h^{-1}$ in the above temperature field. As a design option, moving the fuel injection port downward along the fuel feeding tube was attempted in the modeling to flatten the nonuniform temperature distribution. Figure 4 shows the case where the fuel injection was located at the bottom area of the steam reforming reactor (inner injection). It is not surprising that cold spots shifted down along the injector tube axis as a result of vaporization of liquid. The temperature of the coldest spot in this inner injection mode is about 13°C lower than that in the entrance injection one. The downshifted temperature distribution and the low average catalyst bed temperature result in reduced overall conversion of 90%. The fuel injection location was

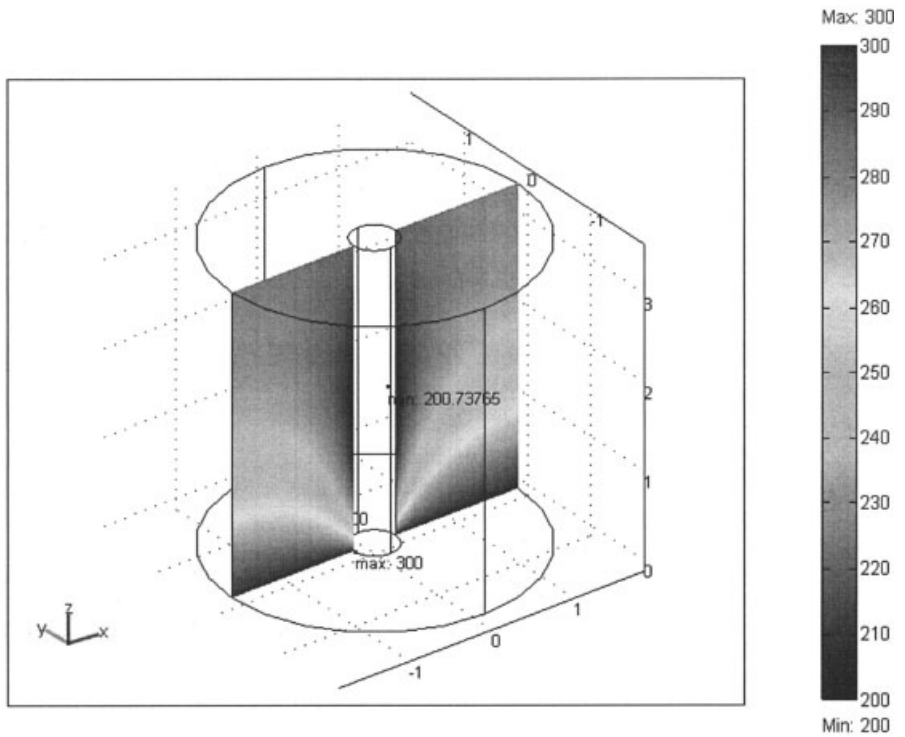

Figure 4. Temperature distribution in a micro-scale methanol steam reformer with a lower injection port.

Conditions: temperature in °C, "adiabatic mode"; $T_{combustion}$ = 300°C, liquid fuel flow rate = 0.05 cm^3/h, steam/C = 1.2.

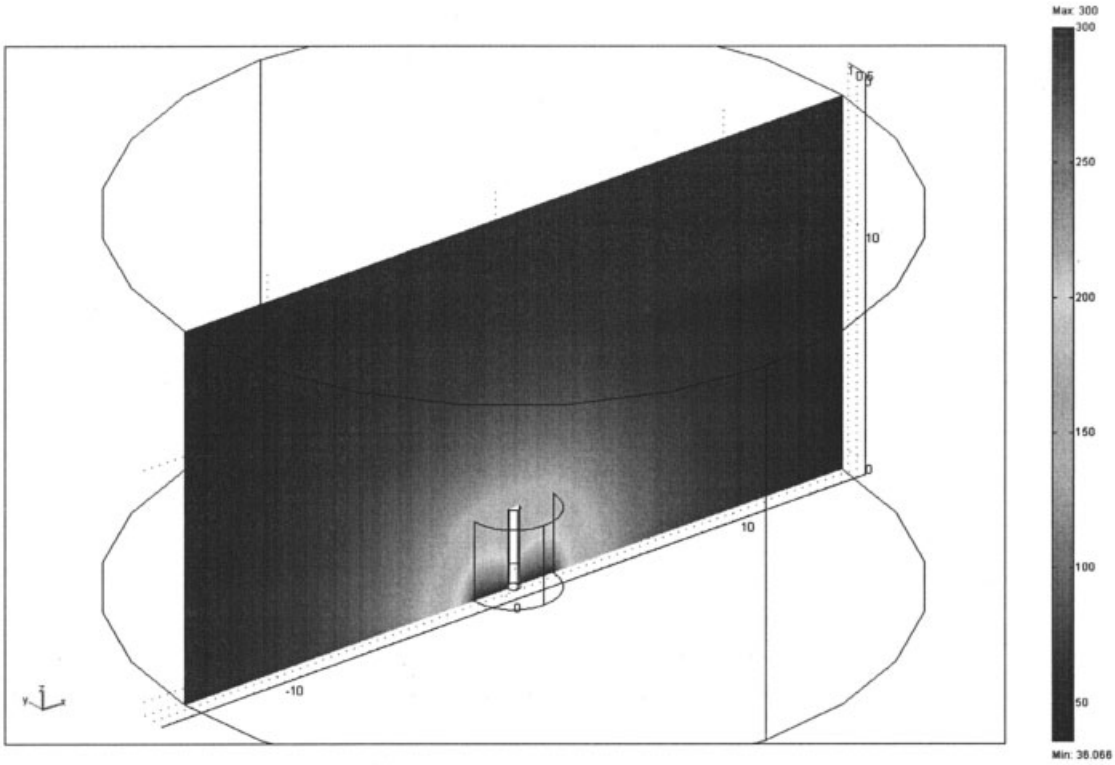

Figure 5. Temperature distribution in a micro-scale methanol steam reformer.

Conditions: temperature in °C, "insulation mode"; fuel injection point: tube inlet; $T_{combustion}$ = 300°C, liquid fuel flow rate = 0.05 cm^3/h, steam/C = 1.2.

optimized in such a way that maximum carbon conversion can be achieved at a relatively uniform temperature distribution. The fuel injection configuration at the inlet has been chosen for the reactor design based on the modeling results.

As indicated in the previous section, heat loss to the environment is an important factor in such a small system. Sufficient insulation is necessary to maintain the desired reaction temperature. However, heavy insulation increases the size and weight of the system, which in turn reduces the power density. An optimized insulation thickness can be determined using the modeling technique. In the computational study, the reformer with an inlet fuel injection configuration was used. Ceramic wool insulation material with a thermal conductivity of 0.028 $W\ m^{-1}\ K^{-1}$ at room temperature was uniformly applied around the reformer with various thicknesses. The natural convection heat transfer coefficient of 5 $W\ m^{-2}\ K^{-1}$ was assigned as a boundary condition with ambient temperature of 22°C. Figure 5 shows the temperature profiles in both the reforming reactor and the insulation domain with 12.7 mm of thickness. The maximum temperature difference within the reformer was found to be 153°C, which is very close to the measured temperature difference 148 °C with the two thermocouples. Compared to the ideal adiabatic steam reformer pellet, the temperature gradient in this realistically insulated reformer is larger because of the heat loss. The skin temperature of the insulation was found to be 50°C, and the heat loss of the entire reformer was 0.58 W out of the methanol combustion heat generation source of 1.39 W. It is observed that energy loss to the environment by convective heat transfer and radiation is substantial compared to the required heat supply of 71.5 mW for fuel vaporization and steam reforming reaction. Subsequently, the thickness of the insulation was varied in the model for optimization. Shown in Figure 6, the simulation results indicate that the skin temperature of the insulated device decreases with the increase of the insulation thickness. However, the total heat loss (W) shows a peak value at the point of 6.35 mm insulation thickness. The less heat loss with thinner insulation (3.175 mm) is attributed to its smaller heat transfer area, although it has a larger driving force and heat transfer coefficient. Thick insulation also results in large surface area that increases the total heat loss. Additionally, the volume of the insulated device must be taken into account so that high energy density can be maintained. Based on the modeling results, the micro-scale reactor design adopted 12.7-mm insulation thickness that gives minimum heat loss, reasonable skin temperature, and acceptable device volume.

The built-in carbon monoxide cleanup portion of the fuel processor was also modeled along with the methanol steam reformer. Because in situ selective methanation reaction was used to convert unwanted CO, hydrogen consumption must be minimized by operating the catalyst at its desired temperature range to reduce CO_2 conversion. Independent fixed-bed testing results for this methanation catalyst showed that the preferred methanation temperature range should be from 250 to 270°C,[12] within which the selectivity to CO conversion reaches a maximum. As shown in Figure 7, the methanator is configured as a "cap" on top of the reformer in the reforming-CO cleanup reactor schemes. Again as a typical example, the simulated

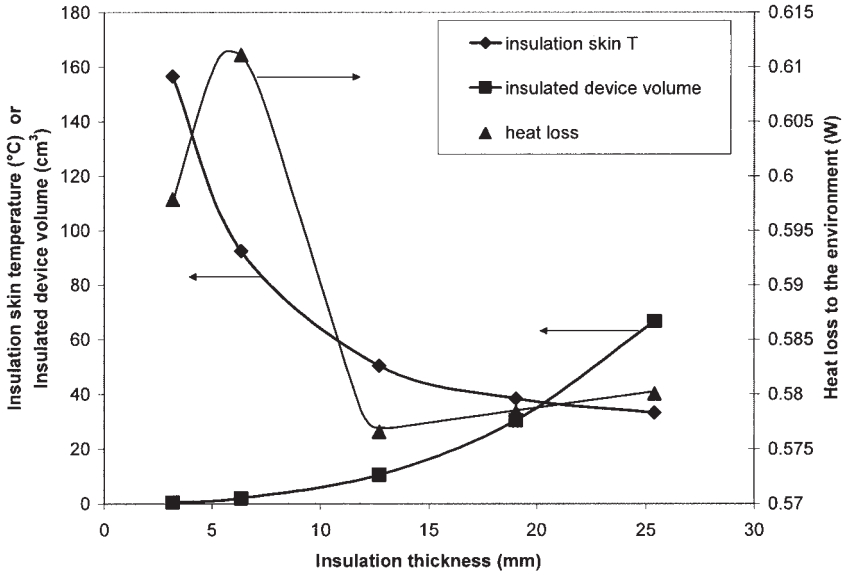

Figure 6. Insulation thickness effect on skin temperature and heat loss.

Conditions: fuel injection point: tube inlet; $T_{combustion}$ = 300°C, liquid fuel flow rate = 0.05 cm^3/h, steam/C = 1.2.

temperature profile shown in Figure 7 corresponds to the conditions of the 80 mW_e output. It is observed that the steam reformer was operated at the temperature range from 270 to 300°C, and the CO methanator at 240–250°C. It has also been found that the heat of methanation reaction was "absorbed" by the latent heat of liquid evaporation with such a configuration. It has been experimentally demonstrated that <100 ppm CO was achieved under the above conditions, but the hydrogen consumption was approximately 15%, which is much higher than the anticipated 7–10%.[5] This indicates that methanation of CO_2 might have also occurred in the catalyst bed, which is possibly at a higher actual temperature. In the future reactor optimization assisted by numerical modeling, the methanation reactor temperature profile could be further tailored and more accurately modeled so that the methanation reactor volume can be adjusted to achieve its maximum performance (low CO ppm and less H_2 consumption).

Conclusion

A three-dimensional (3-D) homogeneous model of catalytic methanol steam reforming and CO methanation reactor for milliwatt-scale hydrogen generation is developed. Partial deferential equations describing conservation laws for mass and energy are solved to show temperature profiles under realistic conditions. Simulation indicates that a temperature gradient as much as 153°C can occur within the methanol steam reforming catalyst bed when operated in the mode of 80 mW electric power output. A tailored temperature profile and an optimized reactor configuration allow operation of catalysts under their preferred conditions. An insulation thickness of 12.7 mm has been selected based on numerical modeling to reduce the heat loss while maintaining small volume and providing high energy density. An optimized fuel injector location has also been determined by numerically evaluating numerous design op-

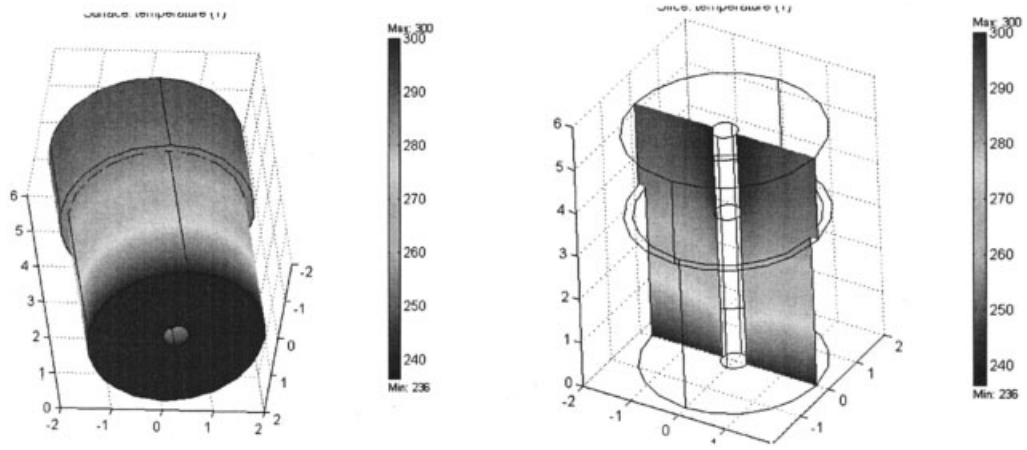

Figure 7. Temperature profiles in a micro-scale methanol steam reformer and selective CO methanator.

Conditions: temperature in °C, "insulation mode"; fuel injection point: tube inlet; $T_{combustion}$ = 300°C, liquid fuel flow rate = 0.05 cm^3/h, steam/C = 1.2)

tions. This model allows adjustment of parameters, such as the preexponential term of the intrinsic rate constant, effective thermal conductivity, and mass diffusivity of the catalyst bed, so that the reactor performance can be simulated with different catalyst activities and selectivities.

Acknowledgments

The authors gratefully acknowledge the sponsorship from the Defense Advanced Research Projects Agency. This work was performed in the Environmental Molecular Sciences Laboratory, a national scientific user facility sponsored by the U.S. Department of Energy's Office of Biological and Environmental Research and located at Pacific Northwest National Laboratory in Richland, WA.

Literature Cited

1. Hossain S. Rechargeable lithium batteries (ambient temperature). In: Linden D, ed. *Handbook of Batteries*. New York, NY: McGraw-Hill; 1995:36.1.
2. Linden D. Selection and application of batteries. In: Linden D, ed. *Handbook of Batteries*. New York, NY: McGraw-Hill; 1995:6.5.
3. Holladay JD, Jones EO, Phelps M, Hu J. Microfuel processor for use in a miniature power supply. *J Power Sources*. 2002;108:21-27.
4. Palo DR, Holladay JD, Jones EO, Rozmiarek RT, Guzman C, Wang Y, Hu J, Dagle RA, Baker EG. Fuel processor development for a soldier-portable fuel cell system. Proc. of IMRET 5 2001 International Conference on Microreaction Technology, Strasbourg, France; 2001.
5. Holladay JD, Jones EO, Dagle RA, Xia GG, Cao C, Wang Y. High efficiency and low carbon monoxide micro-scale methanol processors. *J Power Sources*. 2004;131:69-72.
6. Cao C, Xia G, Holladay J, Jones E, Wang Y. Kinetic studies of methanol-steam reforming over Pd/ZnO catalyst using a microchannel reactor. *Appl Catal A Gen*. 2004;262:19-29.
7. Chin Y, Dagle R, Hu J, Dohnalkova AC, Wang Y. Steam reforming of methanol over highly active Pd/Zno catalyst. *Catal Today*. 2002;77: 79-88.
8. Chin YH, Wang Y, Dagle RA, Li SX. Methanol steam reforming over Pd/ZnO: Catalyst preparation and pretreatment studies *Fuel Process Technol*. 2003;83:193–201.
9. http://www.comsol.com/, 2004.
10. Reid RC, Prausnitz JM, Poling BE. *The Properties of Gases and Liquids* (4th ed.). New York, NY: McGraw-Hill; 1987.
11. Perry RH, Green DW. *Perry's Chemical Engineer's Handbook* (7th ed.). New York, NY: McGraw-Hill; 1997.
12. Dagle RA, Wang Y. Highly active and selective methanation catalysts for fuel processing applications. *Catal Lett*. Submitted.

Manuscript received Mar. 11, 2004, and revision received July 9, 2004.